

Coaxial circular array: Study of farfield pattern and field frequency responses

Bishwajit Chakraborty

National Institute of Oceanography, Dona Paula, Goa 403 004, India

(Received 9 October 1985; accepted for publication 12 December 1985)

A theoretical analysis of vertical farfield patterns for a coaxial circular array of 24 discrete circular radiators has been performed. The narrowest beamwidth (2°) was obtained at an operating wavelength of 0.5λ . A sharp pattern and decreasing directive indices with an increase in the operating wavelength established the suitability of such array geometry for underwater bathymetric applications.

PACS numbers: 43.30.Jx, 43.20.Rz, 43.30.Yj

INTRODUCTION

In the last few years, the study of field patterns for ultrasonic imaging of a transducer array of coaxial circular spherical geometry (Shibata *et al.*¹) has been carried out. The importance of symmetrical as well as narrow-beam angles lies in the fact that we get well-resolved bathymetry through transducer array arrangement for an echo sounder and a sub-bottom profiler.

In view of the above, the present communication deals with the theoretical analysis of coaxial circular array arrangement by slightly modifying the geometrical form, proposed by Shibata *et al.*¹ Three concentric circles of different diameters were chosen on the basis of operating wavelength. Each circle consists of eight elements; hence, a total of 24 elements are distributed within the array system. Each element is assumed to be a circular disk and mutual interactions between the elements are neglected. Vertical farfield patterns for different radii of the middle circle are obtained, keeping the outer and inner radii constant. Along with the above, such arrays are expected to have the property of being frequency independent (Rumsey²). Therefore the vertical farfield for the $\phi = 0^\circ$ plane is presented at different frequencies suitable both for echo sounding and sub-bottom profiling. Directivity indices are calculated from the plotted pattern by employing Elliot's method and are tabulated at different frequency ranges (see Table I).

TABLE I. Directivity indices calculated at different operating wavelengths.

Sl. No.	Operating wavelength in terms of λ	Half-power beam-width (from Fig. 3)	Directivity $D = \frac{32400}{B_x \cdot B_y}$	Directivity indices $DI = 10 \log_{10}(D)$ dB
1.	0.5	2°	8100.00	39.08
2.	1.0	3.3°	2975.20	34.73
3.	1.5	5.3°	1153.40	30.62
4.	2.5	8.6°	438.07	26.42
5.	7.5	26°	47.93	16.81

I. ANALYSIS

Figure 1 shows three circles of different radii on the xy plane. Each element is assumed to be a circular disk with a radius equal to $\lambda/2$, where λ is the operating wavelength. Such assumptions were made for a more practical approach towards the farfield pattern of an array system instead of point-source radiators. Each circle consists of eight elements and a total of 24 radiators are distributed in the array system. The farfield radiation pattern for a coaxial circular system is given by

$$F(\theta, \phi) = f(\theta, \phi) \cdot \text{Element pattern.} \quad (1)$$

A constant multiplying factor in Eq. (1) is, however, being dropped. The array factor $f(\theta, \phi)$ is presented by Collin and Zucker³ as

$$f(\theta, \phi) = \sum_{m=1}^N A_m \exp(j\beta \mathbf{r}_m \cdot \mathbf{R}), \quad (2)$$

where A_m is the complex excitation coefficient which is equivalent to unity in the present case because each radiator is assumed to be excited uniformly and $\beta = 2\pi/\lambda$. In Eq. (2), for the coaxial circular array,

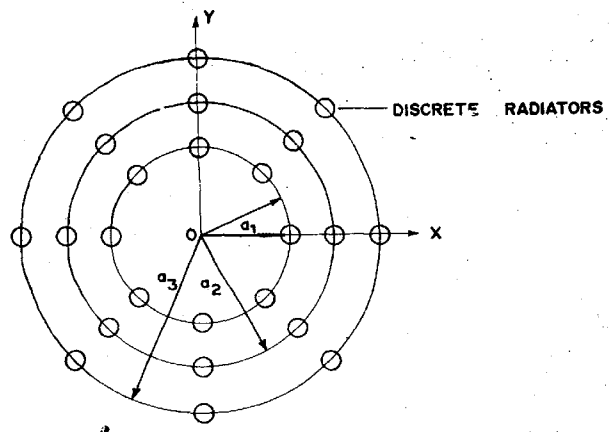


FIG. 1. Geometry of the coaxial circular array.

$$\mathbf{r}_m = x_m \mathbf{i} + y_m \mathbf{j}, \quad (3)$$

where

$$x_m = a \cos(m-1)\pi/4,$$

$$y_m = a \sin(m-1)\pi/4,$$

and \mathbf{i}, \mathbf{j} are unit vectors in their respective directions. The polar unit vector \mathbf{R} can be expressed as

$$\mathbf{R} = (\sin \theta \cos \phi) \mathbf{i} + (\sin \theta \sin \phi) \mathbf{j}. \quad (4)$$

The array factor for a coaxial circular array of a single turn i.e., circular array, can be written as

$$f(\theta, \phi) = \sum_{m=1}^N \exp j\beta [a \sin \theta \cos \phi \cos(m-1)\pi/4 + a \sin \theta \sin \phi \sin(m-1)\pi/4]. \quad (5)$$

Equation (5) is applicable to a single term of the circular array which consists of eight elements. In the present case of a coaxial circular array, there are three such circles of different radii. The radii of the innermost, middle, and outermost circles are expressed as a_1, a_2, a_3 , respectively. Finally, the array factor for three coaxial circles can be written as

$$f(\theta, \phi) = \sum_{m=1}^8 \exp j\beta [a_1 \sin \theta \cos \phi \cos(m-1)\pi/4 + a_1 \sin \theta \sin \phi \sin(m-1)\pi/4] + \sum_{m=9}^{16} \exp j\beta [a_2 \sin \theta \cos \phi \cos(m-1)\pi/4 + a_2 \sin \theta \sin \phi \sin(m-1)\pi/4] + \sum_{m=17}^{24} \exp j\beta [a_3 \sin \theta \cos \phi \cos(m-1)\pi/4 + a_3 \sin \theta \sin \phi \sin(m-1)\pi/4]. \quad (6)$$

In Eq. (1),

$$\text{Element pattern} = \frac{2J_1(\beta \bar{a} \sin \theta)}{\beta \bar{a} \sin \theta}, \quad (7)$$

where J_1 is first-order Bessel function of argument $\beta \bar{a} \sin \theta$ and \bar{a} is the radius of the element and in the present case it is equal to 0.5λ which is assumed to be fixed throughout the analysis. Final expression for the vertical farfield pattern can be obtained by substituting Eqs. (6) and (7) into Eq. (1).

Farfield patterns for fixed outermost and innermost radii of circles of 8.0λ and 4.0λ for three different radii of the middle circle ($5.0\lambda, 6.0\lambda$, and 7.0λ) are shown in Fig. 2. It is clear from Fig. 2 that although the changes in the middle circle radii do not affect the main beamwidth of the farfield pattern, the level of the sidelobe changes accordingly. The main beamwidths (3.3°) are considerably narrow and hence can be useful for many underwater applications. In order to

study the wideband behavior of such array geometry, one of the above combinations ($a_1 = 4.0\lambda, a_2 = 6.0\lambda$, and $a_3 = 8.0\lambda$) of the array is chosen. The narrowest main beamwidth (2°) is obtained for an operating wavelength of 0.5λ and a gradually increasing main beamwidth ($3.3^\circ, 5.3^\circ, 8.6^\circ, 26^\circ$) at $1.0\lambda, 1.5\lambda, 2.5\lambda$, and 7.5λ , respectively. Though an increase in the main beamwidth is observed with a change in operating wavelength, especially 26° at 7.5λ , it will nevertheless be useful for sub-bottom profiling with relative greater area coverage. See Fig. 3.

Elliot (Frank *et al.*, Ref. 4) has developed a method to evaluate the directivity for most general distributors.

$$D = 32\,400/B_x \cdot B_y, \quad (8)$$

where 32 400 is equal to the product of the real beamwidth and the directivity for a planar array at the same tilt angle.

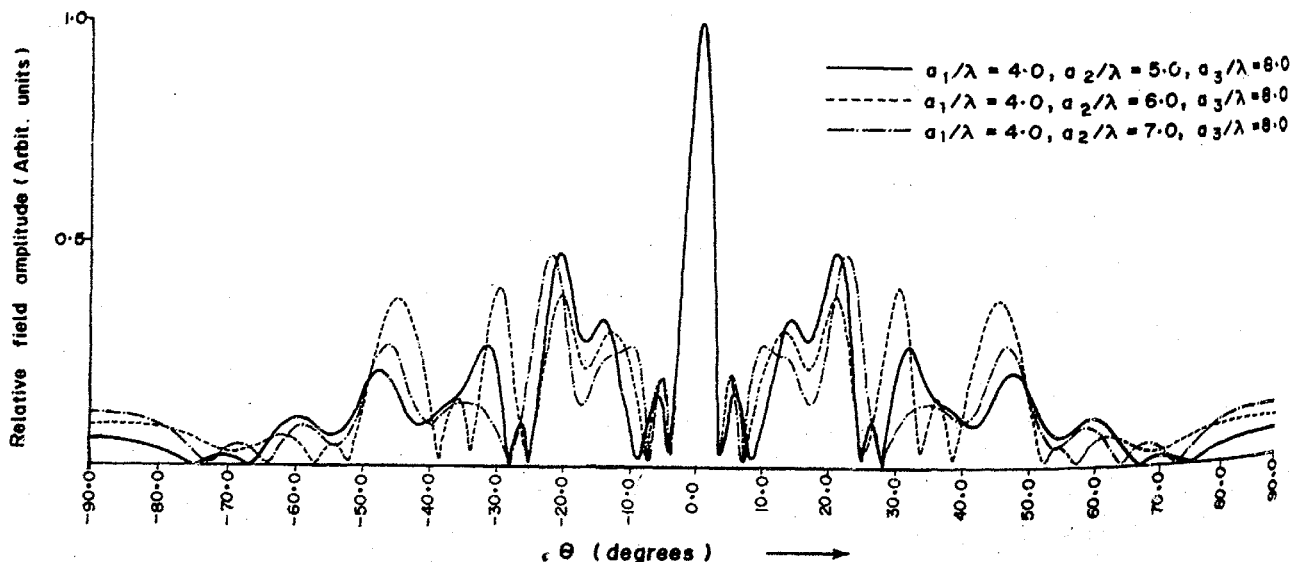


FIG. 2. Vertical farfield pattern for the $\phi = 0^\circ$ plane for three different values of the middle circle radii of the array system.

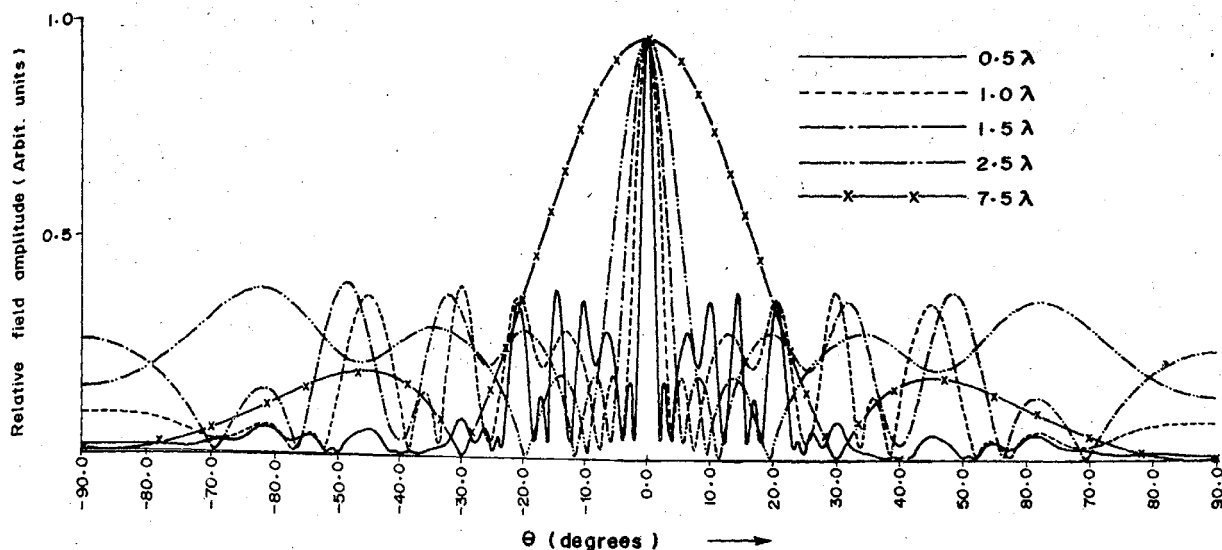


FIG. 3. Vertical farfield pattern for the $\phi = 0^\circ$ plane at five different operating wavelengths.

B_x , B_y are beamwidths along x and y axes, respectively (since structure is symmetrical about the z axis, the beamwidth in the x and y directions are equal). So the directivity indices can be represented by

$$DI = 10 \log_{10}(D). \quad (9)$$

Equation (9) is used to calculate the directivity indices at different frequencies of the array system.

Directivity indices, tabulated for five frequencies, show a fall with increasing operating wavelength which is quite acceptable.

II. CONCLUSIONS

An expression for the farfield pattern is developed for a coaxial circular array with three turns. An observation is made to determine the constancy of the main beamwidth and the fluctuating sidelobe level for the varying middle-circle radius of the geometry. Sharp vertical farfield patterns are obtained at five different frequencies suitable for underwater echo sounding as well as sub-bottom profiling. A sufficiently higher value of the directivity index at the lowest operating wavelength and a gradual fall of directivity indices

with respect to increasing operating wavelength ensures wide applicability of such array geometry for highly resolved bathymetric studies as well as greater coverage.

ACKNOWLEDGMENTS

The author acknowledges the constant encouragement of Dr. H. N. Siddiquie, Director, NIO, during the present work and also would like to thank Dr. C. W. Horton, Sr., Applied Research Laboratory, The University of Texas at Austin, Austin, for his useful suggestions related to present work. Thanks are due to Miss Alison Luis for typing the manuscript.

¹S. Shibata, T. Koda, and J. Yamaga, *J. Acoust. Soc. Am.* **62**, 819-824 (1977).

²V. H. Rumsey, "Frequency independent Antenna," *Inst. Radio Eng. Nat. Convention Rec. Part 1*, **5**, 114-119 (1957).

³R. E. Collin and F. J. Zucker, *Antenna Theory* (McGraw-Hill, New York, 1969), p. 141.

⁴T. H. Frank, J. N. Kesner, and H. M. Gruen, *J. Acoust. Soc. Am.* **63**, 841-847 (1978).